

BioSystems 48 (1998) 147-156



# Investigating spike backpropagation induced Ca<sup>2+</sup> influx in models of hippocampal and cortical pyramidal neurons

Petr Maršálek a,b,\*, Fidel Santamaría c

<sup>a</sup> Department of pathological physiology, 1st Medical Faculty, Charles University, U nemocnice 5, Prague 2, CZ-12853, Czech Republic

<sup>b</sup> A.M. Turing Laboratories, Strimelicka 14, Prague 4, CZ-14100, Czech Republic <sup>c</sup> Computation and Neural Systems Program, 139–74, California Institute of Technology, Pasadena, CA 91125, USA

### Abstract

We modeled the influx of calcium ions into dendrites following active backpropagation of spike trains in a dendritic tree, using compartmental models of anatomically reconstructed pyramidal cells in a GENESIS program. Basic facts of ion channel densities in pyramidal cells were taken into account. The time scale of the backpropagating spike train development was longer than in previous models. We also studied the relationship between intracellular calcium dynamics and membrane voltage. Comparisons were made between two pyramidal cell prototypes and in simplified model. Our results show that: (1) sodium and potassium channels are enough to explain regenerative backpropagating spike trains; (2) intracellular calcium concentration changes are consistent in the range of milliseconds to seconds; (3) the simulations support several experimental observations in both hippocampal and neocortical cells. No additional parameter search optimization was necessary. Compartmental models can be used for investigating the biology of neurons, and then simplified for constructing neural networks. © 1998 Elsevier Science Ireland Ltd. All rights reserved.

Keywords: Active dendrite; Spike backpropagation; Pyramidal cell; Calcium channels; Computational model

### 1. Introduction

The present knowledge of the biology of pyramidal cells extends further than our understanding of their function. Constructing compartmental and simplified models are useful for organizing

experimental data and for inspiring neural network designs. The compartmental models used here are 'canonical', Douglas and Martin, (1990), because they incorporate only a representative selection of elements that seem to dominate pyramidal cells. There was originally the simple view that the dendritic tree in these cells is completely passive, Yuste and Tank, (1996). All compartmental models up to recent times were constructed

<sup>\*</sup> Corresponding author. Tel.: + 420 2 24914929; fax: + 420 2 24912834; e-mail: marsalek@karlin.mff.cuni.cz.

this way, Wathey et al. (1992), Mainen et al. (1995). However, the experimental literature, Turner et al. (1991), Jaffe et al. (1992), Stuart and Sakmann (1994), has begun to report that there are active conductances in the dendritic tree. Independently the theory of single cell biophysics has developed several hypotheses on active dendritic conductances, Mel (1993), Yuste and Tank (1996).

One thing remains common to both passive and active dendritic trees in models and in experiments: the action potential always starts at the axonal hillock. How can this be, with active conductances present in dendrites? Simply, because the density of active conductances governing spike generation is in dendrites different than in the rest of the cell. Channel densities in pyramidal cells are specific in distinct compartments of the cell, Magee and Johnston (1995), Hoffman et al. (1997). The highest densities of sodium channels are at the axonal hillock and in the cell body while a low, but functionally meaningful density is in the rest of the dendritic tree. Sodium and potassium channels cause spike trains to backpropagate into the dendritic tree where calcium channels mediate calcium influx into a cell.

What is the functional difference between a dendritic tree with active conductances, and one without? In both cases, the action potential propagates not only along the axon, but also back to the dendritic tree. At smaller active channel densities, the depolarization wave propagates along a dendrite with a decay. Only at some (saturating) density of active channels the depolarization wave does not decrement. We can speak about the active backpropagation only in cases, when there is a remarkable difference between spike amplitudes in the passive and active dendritic trees. This difference can be shown in models rather than in experiments.

Is there some experimental counterpart to the theoretical observation of a depolarization wave in small branchlets of the dendritic tree? They are not easily accessible to electrodes. There is however, an experimental technique which enables visualization of calcium accumulation within the whole dendritic tree, Schiller et al. (1995, 1997). The aim of the theoretical work presented here is

to show a connection between membrane voltage and intracellular calcium level in analogy to this technique. One purpose of our models is to show the principles and restrictions of our present biophysical knowledge of the dendritic tree. In both hippocampal and neocortical pyramidal cells spike trains backpropagate into the dendritic tree, Helmchen et al. (1996).

### 2. Construction of models in GENESIS

Two detailed morphologies of pyramidal cells were used. The first one, was a neocortical L5 (layer five) neuron, Mainen et al. (1995). The second was a hippocampal CA1 (area one of cornu Ammonis) neuron, Wathey et al. (1992). The differences between the models were in morphologies and channel densities in corresponding cell compartments. Both cells consisted of several hundred dendritic compartments. In the L5 cell the apical dendrite possessed sodium and calcium channels. In the CA1 cell the apical dendrite was divided into two zones. In the proximal part (less than 100  $\mu$ m from the soma) there were sodium, calcium and potassium channels, and in the distal part, only sodium and calcium channels. This is in agreement with the fast repolarization seen in these neurons. Calcium channels were from Traub et al. (1991). For sodium and potassium channels, the parameters were taken from Mainen et al. (1995). The active currents are modeled by Hodgkin-Huxley kinetics. A patch of dendritic membrane is described by system (a spatial variable is here for simplicity omitted):

$$C\frac{\mathrm{d}V_{\mathrm{m}}}{\mathrm{d}t} = \sum_{\mathrm{Ion}} g_{\mathrm{Ion}} m_{\mathrm{Ion}}^{p_{\mathrm{Ion}}} h_{\mathrm{Ion}}^{q_{\mathrm{Ion}}} (V_{\mathrm{m}} - E_{\mathrm{Ion}})$$

$$+ g_{\mathrm{L}}(V_{\mathrm{m}} - E_{\mathrm{L}}) + I(t),$$
for Ion from {Na, K, Ca}
$$\frac{\mathrm{d}j}{\mathrm{d}t} = \frac{s_{j} - j}{\tau_{j}(V_{\mathrm{m}})},$$
(1)

where  $V_{\rm m}$ , C, and I(t) are membrane voltage, capacity, and input current,  $g_{\rm Na}$ ,  $g_{\rm K}$ ,  $g_{\rm Ca}$ , and  $g_{\rm L}$  are maximal ion channel, and 'leakage' conduc-

for j from  $\{m_{Na}, h_{Na}, m_{K}, m_{Ca}, h_{Ca}\}$ 

Table 1
Passive and active membrane properties used in models L5 and CA1

Passive properties			Channel dist	ribution (pS $\mu$ m <sup>-2</sup>	
	L5	CA1		L5	CA1
$R_{\rm m}$ (k $\Omega$ cm <sup>2</sup> ), $\tau_{\rm m}$ (ms) $R_{\rm a}$ ( $\Omega$ cm)	40 200	15.6 75	I. seg.: Soma	$g_{\text{Na}} = 30000$ $g_{\text{Na}} = 30$ : $g_{\text{Na}} = 100$	No I. Seg. $g_{\text{Na}} = 5000; g_{\text{K}} = 2500$
$R_{\rm in}$ (M $\Omega$ ) $E_{\rm rest}$ (mV)	74.2 -66	50 -70	Basal Apical	$g_{\text{Na}} = 50; \ g_{\text{K}} = 100$	$g_{\text{Na}} = 3000$ , $g_{\text{K}} = 2300$ $g_{\text{Na}} = 150$ ; $g_{\text{K}} = 70$ $g_{\text{Na}} = 30$ ; $g_{\text{K}} = 20$ ; P.: $g_{\text{Ca}} = 1$ ;

Passive properties:  $R_{\rm m}$ , membrane resistance. Because membrane capacitance  $C_{\rm m}=1~\mu{\rm F/cm^2}$  in both L5 and CA1, numerically  $R_{\rm m}C_{\rm m}=\tau_{\rm m}=R_{\rm m}$ ;  $R_{\rm a}$ , axial resistance;  $R_{\rm in}$ , input resistance;  $E_{\rm rest}$ , resting potential. Active properties:  $g_{\rm Na}$ ,  $g_{\rm K}$ , and  $g_{\rm Ca}$  are maximal active conductances in given part of the cell.

I.seg., Initial segment; P, The calcium conductance in CA1 (1 pS  $\mu$ m<sup>-2</sup>) was confined to proximal part of the apical dendrite.

tances,  $E_{\rm Na}$ ,  $E_{\rm K}$   $E_{\rm Ca}$ , and  $E_{\rm L}$ , are appropriate equilibrium potentials. The second equation represents the system of five equations for activation and inactivation variables,  $j=m_{\rm Na}$ ,  $h_{\rm Na}$ ,  $m_{\rm K}$ ,  $m_{\rm Ca}$ ,  $h_{\rm Ca}$ , with steady state values  $s_j$ , and time constants  $\tau_j(V_{\rm m})$ , computed as dependent on membrane voltage (see Table 1). For sodium, p=3 and q=1. For sodium, the voltage dependent steady state value of  $s_{\rm Na}=m_{\infty,\rm Na}$  and the appropriate voltage dependent activation time constant  $\tau_{\rm m,Na}$ , are computed as:

$$m_{\infty, \text{Na}} = \frac{\alpha}{\alpha + \beta}$$

$$\tau_{m, \text{Na}} = \frac{1}{\alpha + \beta}$$
(2)

from voltage dependent  $\alpha$ , and  $\beta$  rate parameters:

$$\alpha(V_{\rm m}) = \frac{A(V_{\rm m} - V_{1/2})}{1 - e^{-(V_{\rm m} - V_{1/2})/k}}$$

$$\beta(V_{\rm m}) = \frac{-A(V_{\rm m} - V_{1/2})}{1 - e^{(V_{\rm m} - V_{1/2})/k}},$$
(3)

with  $V_{1/2}$  half activation voltages, k slopes, and A proportional constants of these corresponding Boltzmann functions. Inactivation time constant  $\tau_{\rm h,Na}$  was computed as in Eq. (2), and the inactivation steady state value was:

$$h_{\infty,\text{Na}} = \frac{1}{1 + \rho^{(V_{\text{m}} - V_{1/2})/k}}.$$
 (4)

Further, the potassium current is noninactivating, with p = 1 and q = 0, with time constant, and parameters, as in Eq. (2). See Table 1.

It was concluded from both measurements and simulations, Jaffe et al. (1994), that the density of L- and N-type channels is ten times the density of T-type channels. We used one calcium channel, with properties of both L-, and N-type channels, with inactivating kinetics. These channel kinetics are representative of the values for calcium channels found by other authors, e.g. Reuveni et al. (1993), and Migliore et al. (1995). The calcium channel dynamics were modeled with activation and inactivation as in Traub et al. (1991). The inactivation time constant was fixed,  $\tau_{\rm h,Ca} = 20$  ms. The calcium influx current obeys the standard Hodgkin–Huxley kinetics as well, in this case with p=2 and q=1.  $\alpha_{\rm m,Ca}$  and  $\beta_{\rm m,Ca}$  are:

$$\alpha_{\text{m,Ca}}(V_{\text{m}}) = \frac{A}{1 + e^{-(V_{\text{m}} - V_{1/2})/k}},$$

$$\alpha_{\text{h,Ca}}(V_{\text{m}}) = Ae^{-V_{\text{m}}/k},$$

$$\beta_{\text{h,Ca}}(V_{\text{m}}) = \alpha_{\text{h,Ca}}(0) - \alpha_{\text{h,Ca}}(V_{\text{m}}),$$
(5)

for  $V_{\rm m}>0$ , and  $\alpha_{\rm h_1,Ca}(V_{\rm m})=\alpha_{\rm h_1,Ca}(0)$ , and  $\beta_{\rm h_1,Ca}(V_{\rm m})=0$  for  $V_{\rm m}\leq 0$ .  $\beta_{\rm m,Ca}$  is as in Eq. (3). See Table 2 for numerical values.

Calcium channels contribute to the influx of calcium ions into their intracellular pool. Intracellular calcium,  $[Ca^{2+}]_i$ , is kept low, and thus the driving ion potential is high. Every rise in  $[Ca^{2+}]_i$  is followed by its extrusion by various mechanisms. We used a formalism from Bower and Beeman (1995), where calcium buffering and extrusion are incorporated in one equation. Calcium entering into a given compartment is bound by

Table 2			
Parameters	for	active	conductances

Particles	Constants				Constants		
	$\overline{A}$	k	$V_{1/2}$	Particles	$\overline{A}$	k	$V_{1/2}$
Na, m, α	0.182	9	-35	Κ, m, α	0.02	9	20
Na, <i>m</i> , β	0.124	9	-35	$K, m, \beta$	0.002	9	20
Na, $h$ , $\alpha$	0.24	5	-50	Ca, $m$ , $\alpha$	1.6	-13.9	65
Na, $h$ , $\beta$	0.91	5	-75	Ca, $m$ , $\beta$	0.02	5	-51.1
Na, $h$ , $\alpha$	_	6.2	-65	Ca, $h$ , $\alpha$	0.005	20	_

Parameters used in voltage dependencies of particle activation (m) and inactivation (h) state variables, as given in Eqs. (1)-(5).

the buffer of appropriate size B. (The constant of calcium influx proportionality is  $B_0 = 5$  pMol/ $\mu$ A, and  $B = B_0/V$ , where V is volume of the compartment.) Then calcium ions are subject to extrusion with time constant  $\tau_{\text{Ca}} = 200$  ms:

$$\frac{d[Ca^{2+}]_i}{dt} = -\frac{[Ca^{2+}]_i}{\tau_{Ca}} + BI_{Ca},\tag{6}$$

where  $I_{\rm Ca} = g_{\rm Ca} m_{\rm Ca}^2 h_{\rm Ca} (V_{\rm m} - E_{\rm Ca})$  is the calcium current influx from Eq. (1). The first term on the right side is a summary of all the extrusion mechanisms, fitted to an exponential decay. The second term gives the intracellular calcium increase. No diffusion of intracellular calcium ions was considered because the diffusion time constant is large, compared to the time course of the phenomena studied here.

Our channel densities in L5 were as reported in Mainen et al. (1995) with several additions. In their original model of L5, only a single action potential, AP, with its corresponding back propagating AP were generated and when given a prolonged current step the inactivation inhibited any further generation of AP. In order to be able to generate trains of action potentials with their corresponding backpropagating AP we increased the sodium channel densities in basal dendrites in L5 from 30 pS $\mu$ m<sup>-2</sup> to 50  $pS\mu m^{-2}$ . This yielded appropriate backpropagation of single spike and spike train. Following their model of L5, potassium channels were excluded from the apical dendritic tree in order to maintain slow dendritic repolarization, described by Stuart and Sakmann (1994). A similar procedure was applied in the CA1 model adapted from Wathey et al. (1992). We used a 25  $\mu$ s time step and the Backward Euler method solved with the Hines technique, (Hines, 1984), implemented in GENESIS, Bower and Beeman, (1995).

## 3. Results in compartmental models

The first section deals with fitting the model to produce a backpropagating spike train. The other two sections deal with calcium dynamics in the apical trunk.

### 3.1. Spike backpropagation

A constant supra-threshold current injection was applied to the soma of each neuron eliciting a spike train. This train backpropagated into the dendritic tree. The APs originated at the initial axon segment near the soma and backpropagated to the dendritic tree. In both models (hippocampal and neocortical) the maximal voltage of the AP as a function of distance from the soma (measured along the dendrite), exhibits a second peak at distal dendritic tips (consistent with Yuste et al., 1994, Schiller et al., 1997). The firing frequency of the model is increased, compared to the model modification without active channels (not shown). The attenuation of APs after the first spike was also observed. Fig. 1 shows different levels of inactivation along the apical trunk after a train of APs is elicited at the soma. The first spike is barely attenuated

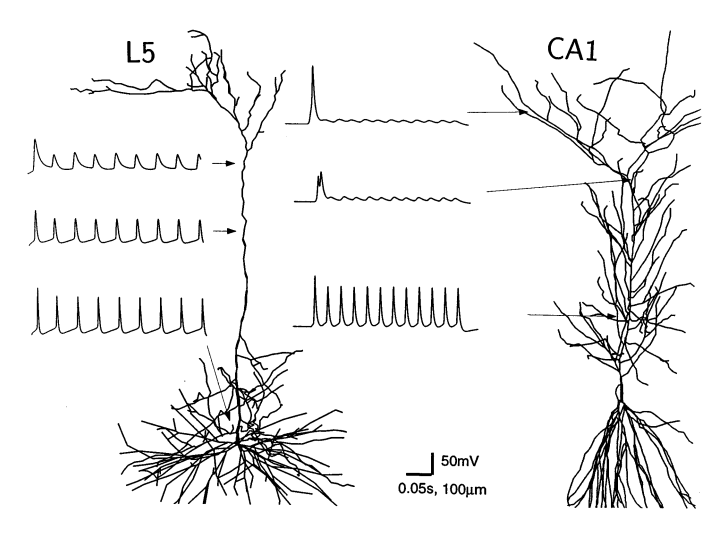


Fig. 1. Firing of reconstructed cells at three different distances from the soma. Sustained (DC) current (0.5 nA in L5 and 0.17 nA in CA1) was injected at the soma. In the more branched hippocampal cell, AP amplitude decrement along one principal dendrite is more dramatic.

but the following are attenuated proportionally to the distance.

# 3.2. Intra-cellular calcium, accumulation related to geometry

We investigated the spatiotemporal profile of calcium accumulation following a backpropagating spike train. The aim was to see whether calcium influx through calcium channels is determined by the spread of action potentials, as proposed by Spruston et al. (1995). In agreement with several experimental observations Jaffe et al. (1994), Migliore et al. (1995) (and in order to reduce the complexity of the model), the calcium channel density was uniform throughout the dendritic tree.

The calcium accumulation plotted against the distance from the soma exhibits a peak along the apical dendrite, as observed by Yuste et al. (1994) in slice experiments. The presence of one, or more peaks in their report are indeed inhomogeneities in calcium accumulation. Both of our models reproduced corresponding nonmonotonic calcium accumulation (Fig. 2), thus demonstrating that cells with uniform channel density accumulate calcium inhomogeneously due to the particular shape of the dendritic tree.

# 3.3. Intra-cellular calcium, its dynamics in apical dendrite

A slice study of [Ca<sup>2+</sup>], level in the proximal apical dendrite following generation of an AP at the soma of pyramidal cells has reported that [Ca<sup>2+</sup>], follows (or encodes) the instantaneous frequency of the spike train Helmchen et al. (1996). In the model we see that the  $[Ca^{2+}]_i$  at the proximal portion of the apical dendrite follows the instantaneous firing at the soma. On the other hand, if we look at the same variable in a distal portion of apical dendrite we see a totally different behavior. Calcium starts to accumulate abruptly following backpropagating spike train and its level is saturated even after a few backpropagating spikes, or even at low cell firing frequencies. Synergy of sodium and calcium channels in distal portion of dendritic tree yields the same dynamics, as described by Jaffe et al. (1992) in experiment. In the proximal apical dendrite successive action potentials in the spike train attenuate minimally. Since each spike contributes an equal amount to the calcium influx, the calcium level in proximal apical dendrite integrates the instantaneous frequency, as demonstrated by Helmchen et al. (1996).

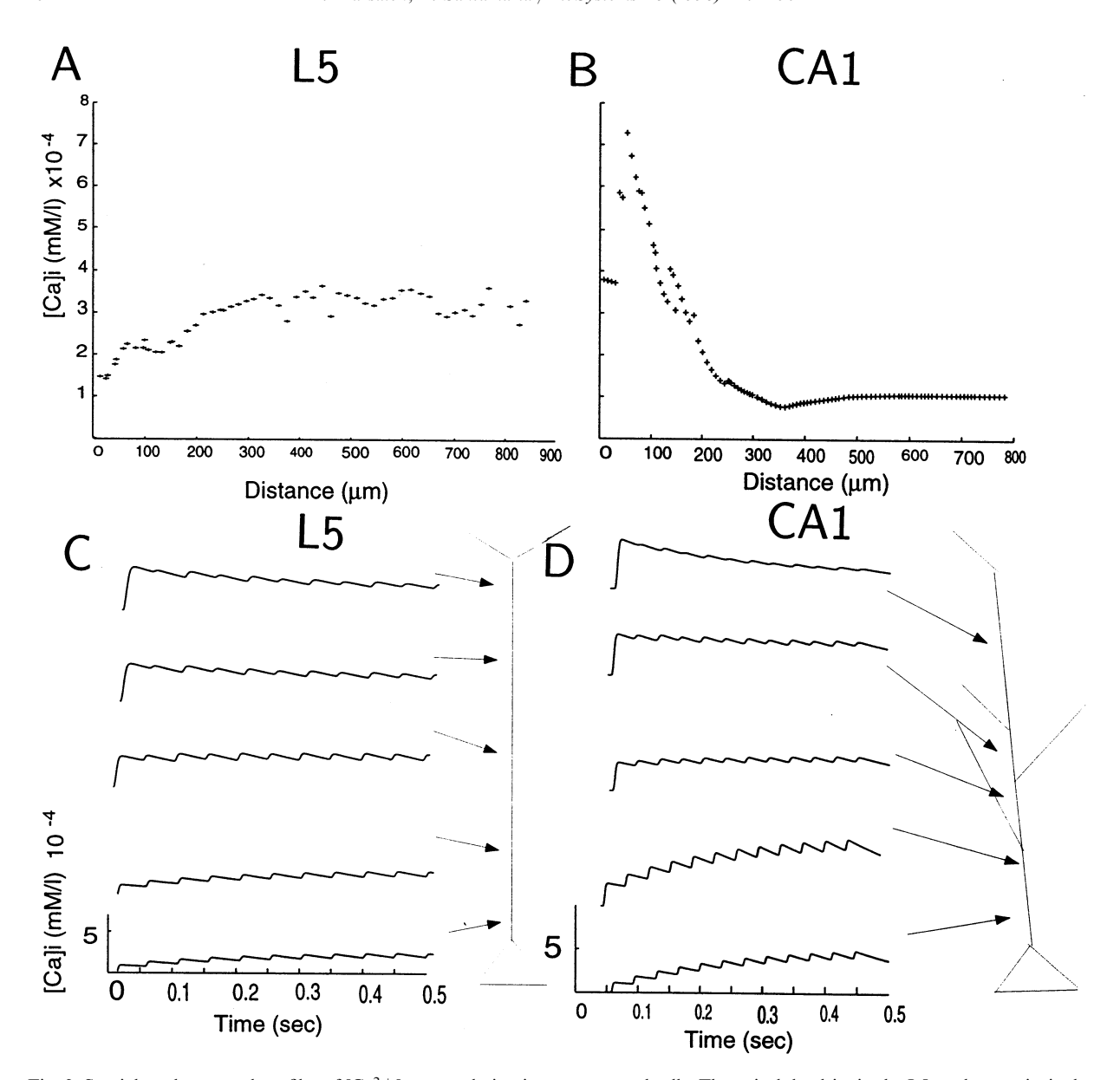


Fig. 2. Spatial, and temporal profiles of  $[Ca^{2+}]_i$  accumulation in reconstructed cells. The apical dendrite in the L5, and one principal dendrite in the CA1 are picked up. A, B, the  $[Ca^{2+}]_i$  level reached after DC stimulus (see Fig. 1). C, D, time evolution of  $[Ca^{2+}]_i$  is plotted at five various distances from the soma. Note that the  $[Ca^{2+}]_i$  scale in A, B is larger than in C, D.

# 4. Results in simplified model

In our simplified model we demonstrate the properties of a neuron's biophysical system that generate dynamics of  $[Ca^{2+}]_i$ . Fig. 3 shows the comparison of calcium accumulation in the proxi-

mal apical dendrite, in the distal part of the dendritic tree (in L5 cell), and in the simplified (or reduced) model, as well. The stimulus was generated following Mainen and Sejnowski (1995) and applied as a current injection. The simplified model is constructed from two RC-circuits (cir-

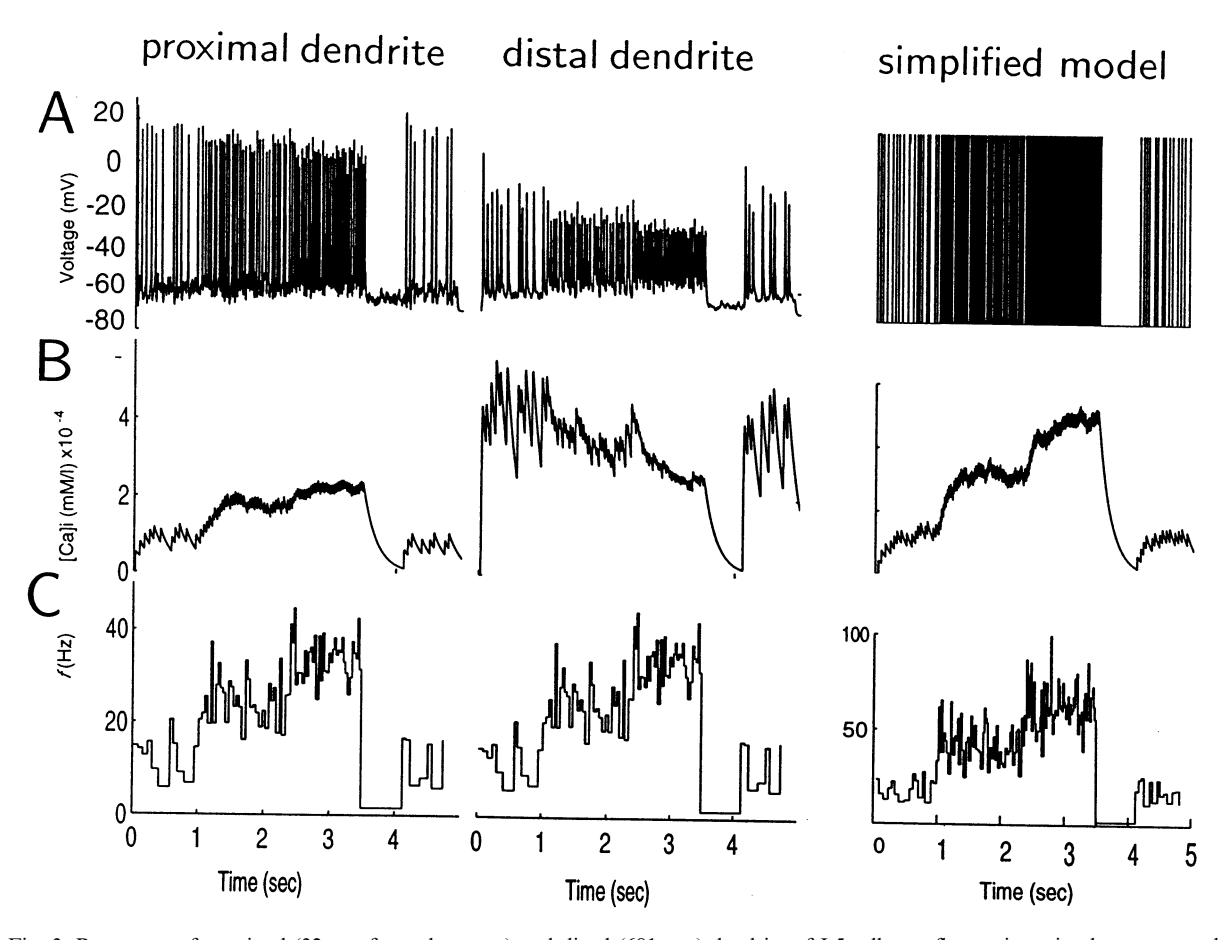


Fig. 3. Responses of proximal (32  $\mu$ m from the soma) and distal (681  $\mu$ m) dendrite of L5 cell to a fluctuating stimulus, compared to the corresponding output of the simplified model. The input was a filtered inhomogeneous Poissonian train of current pulses with successively higher rates (low-pass filtered,  $\tau = 3$  ms). A: action potentials (in the simplified model in arbitrary units). B:  $[Ca^{2+}]_i$  levels. C: instantaneous firing rate.

cuits with resistor and capacitor) using the observation that the calcium decay can be fitted to an exponential function with an appropriate time constant Bower and Beeman (1995), Helmchen et al. (1996). We reduce the spike generation mechanism to a similar equation as in Helmchen et al. (1996), arriving at the following system:

$$\frac{dV}{dt} = -\frac{V_{\rm m}}{\tau_{\rm RC}} + \frac{I_{\rm m}(t)}{C_{\rm m}}, \quad \text{for } V_{\rm m}(t) < V_{\rm th}$$

$$V_{\rm m}(t+dt) = 0, \quad \text{for } V_{\rm m}(t) \ge V_{\rm th}$$

$$\frac{d[Ca^{2+}]_{i}}{dt} = -\frac{[Ca^{2+}]_{i}}{\tau_{Ca}} + \frac{H(V_{\rm m}(t) - V_{\rm Ca})}{C_{Ca}}, \tag{7}$$

where current input  $I_{\rm m}$  to the first equation yields output  $V_{\rm m}$ , which is then used as the input to the second equation to yield the output  $[{\rm Ca^{2+}}]_i$ . Both these equations are nonlinear, because they are endowed with a threshold. The first equation is the well known 'leaky integrator' with threshold  $V_{\rm th}$  Tuckwell (1988), with time constant  $\tau_{\rm RC}$  and capacitance  $C_{\rm m}$ . Calcium influx in the second equation is then determined by  $V_{\rm m}$  exceeding the threshold  $V_{\rm Ca}$  (and rectified by H(t)=0, for t<0, H(t)=1 for  $t\geq0$ , Heaviside step function).  $C_{\rm Ca}$  then scales a calcium buffering capacity and  $\tau_{\rm Ca}$  is the calcium extrusion constant.  $\tau_{\rm Ca}$  is slower compared to  $\tau_{\rm RC}$ . This model extracts the property of

integration of firing rate by calcium level, as shown in Fig. 3. The important parameters of the simplified model are the time constants. From their values we can infer how the activity of a biophysically described neuron can be traced on both a millisecond and a second time scale.

### 5. Discussion

We used two compartmental and one simplified model that have qualitatively reproduced several different physiological phenomena: backpropagating spike trains, spatial calcium accumulation, and the relation of  $[Ca^{2+}]_i$  to the firing rate in proximal apical dendrites. For the latter we suggest using a simplified model consisting of two RC circuits. We have found that the level reached by calcium depends on the diameter and distance from the soma. We have to point out here that these results were generated using a semi-quantitative approach given the diversity of the preparations used in the physiological experiments.

The construction of our models began as a reproduction of the study by Mainen et al. (1995). We added the constraint of regenerative firing in addition to the constraint that the AP is always generated at the soma. Compared to the model of Mainen et al. (1995), and other model by Rapp et al. (1996), the repetitive firing of our model is given by the increment of sodium channels in basal dendrites. A possible experiment could be to study the influence of basal dendrites as a modulator of the backpropagating action potentials by inhibiting or exciting these dendrites.

Opening of the sodium and calcium channels depolarizes the membrane. The density of sodium channels is higher (see Table 1), and therefore their contribution to the depolarization dominates, as shown by Schiller et al. (1997) as well. In the model, after disconnecting calcium channels, repetitive spike generation was not affected (not shown). Repetitive spiking is generated by both sodium and potassium channels. Whether the potassium channels are present in apical dendrites is discussed throughout the literature. We placed them in the proximal part of the apical dendrite of the CA1 case in order to have a fast spike repolar-

ization (in contrast to the slow one observed in the L5 case), following previous models. Their presence in distal dendrites leads to more pronounced regenerative events, as shown in the experiment by Hoffman et al. (1997).

Calcium channels are the most diverse group. Several types are described on pyramidal neurons. Our aim was to show the dynamics of  $[Ca^{2+}]_i$ . We kept our assumptions simple, calcium channels were represented by the most dominant type (uniformity of calcium mechanisms) and their density was homogeneous. We have shown that under this simplest condition, calcium accumulation is inhomogeneous, and depends on a geometry of dendritic tree. Some authors, Helmchen et al. (1996) in L5 and CA1, and Regehr and Tank (1992) in CA1, have found the homogeneity assumption in modeling quite acceptable. Experiments are revealing the further complexity of distribution of these channels in dendritic tree. Svoboda et al. (1997) reports a homogeneous density in vivo. Schiller et al. (1997), together with Stuart et al. (1997), comments in her excellent in vitro results, why the in vivo setup by Svoboda et al. (1997) did not detect inhomogeneous density. We find both the homogeneous and inhomogeneous assumptions reasonable, depending on the level of detail addressed in the biophysical description. For the sake of discussion of channel kinetics we refer further to Magee and Johnston (1995), Colbert and Johnston (1996), Tsubokawa and Ross (1996, 1997) and Hoffman et al. (1997).

We reproduced the observation of Helmchen et al. (1996) on calcium dynamics in proximal apical dendrites. In addition, we studied the calcium dynamics in the distal portion. In distal dendrites, the spike train does not encode instantaneous frequency. Only large variations, and a new spike after a silence period, are reflected. This is caused by the inactivation of ion channels after the first backpropagating AP.

According to Yuste et al. (1994), Spruston et al. (1995), different calcium levels in different branches of the dendritic tree can look like all-ornone events or 'calcium switching' in dendrites. They can be discontinuous, even when the changes of membrane potential in the neighbourhood of branching points are continuous. A biophysical analysis of AP amplitude attenuation

with distance and under various stimulation paradigms is in Migliore (1996). The attenuation depends both on densities of active channels and on dendritic geometry. The amplitude of the AP may be amplified in distal portions of the dendritic tree.

Another experimental investigation of [Ca<sup>2+</sup>], transients in CA1 is in Callaway and Ross (1995). They support their experiment with a simulation of a one-point model of calcium accumulation in dendrites. They arrive at a similar conclusion as we do with our simplified model, Eq. (7), and as the calcium transients modeled in Helmchen et al. (1996). We propose that a new 'integrate and fire' neuron can be defined. This system will be composed of two RC circuits, the first one will be the usual voltage integrator and the second the calcium level integrator, which will encode the instantaneous frequency. The most straightforward way of constructing more complex artificial neurons would be to compose them from several compartments using this system of equations. With these elements it would be easier to implement neural networks obeying learning rules.

### Acknowledgements

Thanks to D. Amaral, F. Bochníček, A. Borst, J. Bower, A. Fenton, G.R. Holt, D.T. Kewley, C. Koch, J. Kofránek, Z. Kučerová, W.W. Lytton, Z. Mainen, R. Murphy, J.-P. Rospars, D.K. Smetters, N. Spruston. We used software packages GENESIS and Matlab. P.M. was supported by NIMH Center for Neuroscience Research at Caltech, and partially by the Internal Grant of the Charles University, number 242/1995 and F.S. was partially supported by the Charles Lee Powel Graduate Foundation.

### References

- Bower, J.M., Beeman, D., 1995. The book of GENESIS. Springer-Verlag, New York.
- Callaway, J.C., Ross, W.N., 1995. Frequency-dependent propagation of sodium action potentials in dendrites of hippocampal CA1 pyramidal neurons. J. Neurophysiol. 74, 1395–1403.

- Colbert, C.M., Johnston, D., 1996. Axonal action-potential initiation and Na<sup>+</sup> channel densities in the soma and axon initial segment of subicular pyramidal neurons. J. Neurosci. 16, 6676–6686.
- Douglas, R., Martin, K., 1990. Neocortex. In: Shepherd G. (Ed.), The Synaptic Organization of the Brain, 2nd ed. Oxford University Press, Oxford, pp. 389–438.
- Helmchen, F., Imoto, K., Sakmann, B., 1996. Ca<sup>2+</sup> buffering and action potential-evoked Ca<sup>2+</sup> signalling in dendrites of pyramidal neurons. Biophys. J. 70, 1069–1081.
- Hines, M., 1984. Efficient computation of branched nerve equations. Int. J. Biomed. Comput. 15, 69–79.
- Hoffman, D.A., Magee, J.C., Colbert, C.M., Johnston, D., 1997. K<sup>+</sup> channel regulation of signal propagation in dendrites of hippocampal pyramidal neurons. Nature 387, 869–875.
- Jaffe, D.B., Johnston, D., Lasser-Ross, N., Lisman, J.E., Miyakawa, H., Ross, W.E., 1992. The spread of Na<sup>+</sup> spikes determines the pattern of dendritic Ca<sup>2+</sup> entry into hippocampal neurons. Nature 357, 244–246.
- Jaffe, D.B., Ross, W.N., Lisman, J.E., Lasser-Ross, N., Miyakawa, H., Johnston, D., 1994. A model for dendritic Ca<sup>2+</sup> accumulation in hippocampal pyramidal neurons based on fluorescence imaging measurements. J. Neurophysiol. 71, 1065–1077.
- Magee, J.C., Johnston, D., 1995. Characterization of single voltage-gated Na<sup>+</sup> and Ca<sup>2+</sup> channels in apical dendrites of rat CA1 pyramidal neurons. J. Physiol. 487 (1), 67–90.
- Mainen, Z., Joerges, J., Huguenard, J.R., Sejnowski, T., 1995.
  A model of spike initiation in neocortical neurons. Neuron 15, 1427–1439.
- Mainen, Z., Sejnowski, T., 1995. Reliability of spike timing in neocortical neurons. Science 268, 1503–1506.
- Mel, B.W., 1993. Synaptic integration in an excitable dendritic tree. J. Neurophysiol. 70, 1086–1101.
- Migliore, M., 1996. Modeling the attenuation and failure of action potentials in the dendrites of hippocampal neurons. Biophys. J. 71, 2394–2404.
- Migliore, M., Cook, E.P., Jaffe, D.B., Turner, D.A., Johnston, D., 1995. Computer simulations of morphologically reconstructed CA3 hippocampal neurons. J. Neurophysiol. 73, 1157–1168.
- Rapp, M., Yarom, Y., Segev, I., 1996. Modeling back propagating action-potential in weakly excitable dendrites of neocortical pyramidal cell. Proc. Natl. Acad. Sci. USA 93, 11985–11990.
- Regehr, W.G., Tank, D.W., 1992. Calcium-concentration dynamics produced by synaptic activation of CA1 hippocampal pyramidal cells. J. Neurosci. 12, 4202–4223.
- Reuveni, I., Friedman, A., Amitai, Y., Gutnick, M.J., 1993. Stepwise repolarization from Ca<sup>2+</sup> plateaus in neocortical pyramidal cells: evidence for nonhomogenous distribution of HVA Ca<sup>2+</sup> channels in dendrites. J. Neurosci. 13, 4609–4621.
- Schiller, J., Helmchen, F., Sakmann, B., 1995. Spatial profile of dendritic calcium transients evoked by action potentials in rat neocortical pyramidal neurones. J. Physiol. 487 (3), 583–600.

- Schiller, J., Schiller, Y., Stuart, G., Sakmann, B., 1997. Calcium action potentials restricted to distal apical dendrites of rat neocortical pyramidal neurons. J. Physiol. 505 (3), 605–616.
- Spruston, N., Schiller, Y., Stuart, G., Sakmann, B., 1995. Activity-dependent action potential invasion and calcium influx into hippocampal CA1 dendrites. Science 268, 297– 300.
- Stuart, G., Schiller, J., Sakmann, B., 1997. Action potential initiation and propagation in rat neocortical pyramidal neurons. J. Physiol. 505 (3), 617–632.
- Stuart, G., Sakmann, B., 1994. Active propagation of somatic action potentials into neocortical pyramidal cell dendrites. Nature 367, 69–72.
- Svoboda, K., Denk, W., Kleinfeld, D., Tank, D.W., 1997. In vivo dendritic calcium dynamics in neocortical pyramidal neurons. Nature 385, 161–165.
- Traub, R.D., Wong, R.K.S., Miles, R., Michelson, H., 1991.
  A model of a CA3 hippocampal pyramidal neuron incorporating voltage-clamp data on intrinsic conductance. J. Neurophysiol 66, 635–650.
- Tsubokawa, H., Ross, W.N., 1996. IPSPs modulate spike backpropagation and associated [Ca<sup>2+</sup>], changes in the

- dendrites of hippocampal CA1 pyramidal neurons. J. Neurophysiol. 76, 2896–2906.
- Tsubokawa, H., Ross, W.N., 1997. Muscarinic modulation of spike backpropagation in the apical dendrites of hippocampal CA1 pyramidal neurons. J. Neurosci. 17, 5782–5791.
- Tuckwell, H.C., 1988. Introduction to Theoretical Neurobiology, vols. 1–2. Cambridge University Press, New York.
- Turner, R.W., Meyers, D.E.R., Richardson, T.L., Barker, J.L., 1991. The site for initiation of action-potential discharge over the somatodendritic axis of rat hippocampal CA1 pyramidal neurons. J. Neurosci. 11, 2270–2280.
- Wathey, J.C., Lytton, W.W., Jester, J.M., Sejnowski, T.J., 1992. Computer simulations of EPSP-spike (E-S) potentiation in hippocampal CA1 pyramidal cells. J. Neurosci. 12, 607–618.
- Yuste, R., Gutnick, M.J., Saar, D., Delaney, K.R., Tank, D.W., 1994. Ca<sup>2+</sup> accumulation in dendrites of neocortical pyramidal neurons: an apical band and evidence for two functional compartments. Neuron 13, 23–43.
- Yuste, R., Tank, D.W., 1996. Dendritic integration in mammalian neurons; a century after Cajal. Neuron 16, 701– 716.